

Search for α -cluster states in even-even Cr isotopes

M. A. Souza^{1,2,*} and H. Miyake^{1,†}

¹*Instituto de Física, Universidade de São Paulo, Rua do Matão,
1371, CEP 05508-090, Cidade Universitária, São Paulo - SP, Brazil*

²*Instituto Federal de Educação, Ciência e Tecnologia de São Paulo - Campus São Paulo,
Rua Pedro Vicente, 625, CEP 01109-010, Canindé, São Paulo - SP, Brazil*

The α + core structure is investigated in even-even Cr isotopes from the viewpoint of the local potential model. The comparison of Q_α/A values for even-even Cr isotopes and even-even $A = 46, 54, 56, 58$ isobars indicates that ^{46}Cr and ^{54}Cr are the most favorable even-even Cr isotopes for α -clustering. The ground state bands of the two Cr isotopes are calculated through a local α + core potential with two variable parameters. The calculated spectra give a very good description of most experimental ^{46}Cr and ^{54}Cr levels. The reduced α -widths, rms intercluster separations and $B(E2)$ transition rates are determined for the ground state bands. The calculations reproduce the order of magnitude of the available experimental $B(E2)$ values without using effective charges and indicate that the first members of the ground state bands present a stronger α -cluster character. The volume integral per nucleon pair and rms radius obtained for the $\alpha+^{50}\text{Ti}$ potential are consistent with those reported previously in the analysis of α elastic scattering on ^{50}Ti .

PACS numbers: 21.60.Gx, 27.40.+z, 23.20.-g, 25.55.Ci

I. INTRODUCTION

The α -cluster structure is present in nuclei of different mass regions and is matter of discussions with many different approaches. A comprehensive review of this research theme, as well as the nuclear clustering in general, is found in Ref. [1], and recent advances are described in Refs. [1, 2]. The α -cluster model has been successful in describing energy levels, electromagnetic transition strengths, α -decay widths and α -particle elastic scattering data. Previous studies [3, 4] have questioned whether the most likely cluster + core structures are determined strictly by the doubly closed shell for cluster and core. Our recent article [5] shows that the local potential model (LPM) with the α + core interpretation can be applied systematically in intermediate mass nuclei around the double shell closure at ^{90}Zr , obtaining a good description of the energy levels and orders of magnitude of the $B(E2)$ transition rates without the use of effective charges. Additionally, Ref. [5] shows that the α + core potential employed in ^{94}Mo and ^{96}Ru are similar to the real parts of the optical potentials used in other studies for analysis of $\alpha+^{90}\text{Zr}$ and $\alpha+^{92}\text{Mo}$ elastic scattering, respectively.

In the fp -shell region, ^{44}Ti is one of the most studied nuclei with the α + core interpretation, since it has the configuration of α -particle plus ^{40}Ca doubly magic core. Works on the $\alpha+^{40}\text{Ca}$ structure in ^{44}Ti (examples in Refs. [6–10]) show good descriptions of the ground state band and $B(E2)$ transition rates. Neighboring nuclei as ^{43}Sc , ^{43}Ti , and others at the beginning of the fp -shell have been analyzed with the LPM [11, 12], however, considering the effect of noncentral forces that arise with non-zero spin cores. The α + core structure in the

fp -shell region has also been examined in nuclei as ^{42}Ca and ^{43}Sc from the viewpoint of the orthogonality condition model [13, 14] and deformed-basis antisymmetrized molecular dynamics [15] with favorable results.

The motivation of this work is the investigation of the α + core structure in nuclei of the Cr isotopic chain, which is near the well-studied ^{44}Ti and presents even-even nuclei without the α + {doubly closed shell core} configuration. The structure of the Cr isotopes has been analyzed in previous studies with different approaches, such as the shell-model and its variations [16–18], Hartree-Fock or Hartree-Fock-Bogoliubov models [19–22], and proton-neutron interacting boson model [18]. Also, the ^{48}Cr nucleus has been described by the $^{40}\text{Ca}+\alpha+\alpha$ structure with the use of the generator coordinate method [23] and orthogonality condition model [24]. Recently, T. Togashi *et al.* [17] investigated natural and unnatural-parity states in neutron-rich Cr and Fe isotopes using large-scale shell-model calculations, obtaining good agreement with experimental energy levels. K. Kaneko *et al.* [16] analyzed neutron-rich Cr nuclei using the spherical shell model; the results give a good general description of the experimental energy levels, and the experimental $B(E2; 2_1^+ \rightarrow 0_1^+)$ values for ^{52}Cr and ^{54}Cr are well reproduced by using effective charges $e_\pi = 1.5e$ and $e_\nu = 0.5e$.

The nuclei of the Cr region have been intensively studied in recent years, since changes in the nuclear shell structure have been observed with the increase of neutron number in the isotopic chain, raising a question about the persistence of the traditional magic numbers in neutron-rich nuclei of the fp -shell. A subshell closure at $N = 32$ is indicated by new measurements of nuclear masses, high 2_1^+ energy levels, and low $B(E2; 0_1^+ \rightarrow 2_1^+)$ values in nuclei as ^{52}Ca [25, 26], ^{54}Ti [27, 28], and ^{56}Cr [29, 30] compared with neighboring isotopes, and a subshell closure at $N = 34$ has been observed in ^{54}Ca [31]. Different studies [16, 18, 32, 33] aim for an increase of collectivity for

* marsouza@if.usp.br

† miyake@if.usp.br

neutron-rich nuclei in the fp -shell region near $N = 40$. In this context, the present work contributes to further discussions on the nuclear structure of this region.

The next section describes a criterion for selection of the preferential nuclei for α -clustering in the set of even-even Cr isotopes. In Section III, the α -cluster model and $\alpha + \text{core}$ potential are described in detail. In Section IV, an analysis of the selected nuclei (^{46}Cr and ^{54}Cr) is presented from the standpoint of the LPM. Conclusions are shown in Section V.

II. SELECTION OF PREFERENTIAL NUCLEI FOR α -CLUSTERING

A preliminary question is the choice of a criterion to determine the most favorable nuclei for α -clustering in a specified set of nuclei. We use the same criterion employed in our previous work [5] which is based only on experimental data of binding energy [34, 35]. An appropriate quantity for comparing different nuclei is the variation of average binding energy per nucleon of the system due to the $\alpha + \text{core}$ decomposition. This value is given by

$$\frac{Q_\alpha}{A_T} = \frac{B_\alpha + B_{\text{core}} - B_T}{A_T}, \quad (1)$$

where Q_α is the Q -value for α -separation, A_T is the mass number of the total nucleus and B_α , B_{core} and B_T are the experimental binding energies of the α -cluster, the core and the total nucleus, respectively. Thus, an absolute (or local) maximum of Q_α/A_T indicates the preferred nucleus for α -clustering in comparison with the rest of (or neighbouring) nuclei in the set.

This study focuses mainly on the comparison of Cr isotopes. FIG. 1 shows graphically the values of Q_α/A_T for even-even Cr isotopes, where there are two Q_α/A_T peaks for ^{46}Cr (≈ -147.7 keV) and ^{54}Cr (≈ -146.8 keV). These nuclei correspond to ^{42}Ti and ^{50}Ti cores with magic numbers of neutrons $N = 20$ and $N = 28$, respectively. However, the ^{56}Cr and ^{58}Cr isotopes have Q_α/A_T values (≈ -147.1 keV and -149.4 keV, respectively) very close to those of ^{46}Cr and ^{54}Cr . This feature suggests the influence of a neutron subshell closure above $N = 28$ for the core. In the case of ^{58}Cr , there is a ^{54}Ti core with $N_{\text{core}} = 32$, which is related to a subshell closure as discussed in previous studies (see Section I).

FIG. 2 shows graphically the values of Q_α/A_T for even-even $A = 46, 54, 56, 58$ isobars. An absolute Q_α/A_T peak is seen to ^{46}Cr in the $A = 46$ graph, and a local peak is seen for ^{54}Cr in the $A = 54$ graph. However, the ^{56}Cr and ^{58}Cr nuclei do not correspond to absolute or local maxima of Q_α/A_T in the $A = 56$ and $A = 58$ graphs. Therefore, an overall evaluation of the Q_α/A_T values in FIGS. 1 and 2 implies that ^{46}Cr and ^{54}Cr are preferential nuclei for α -clustering if they are compared with other even-even Cr isotopes and respective even-even isobars

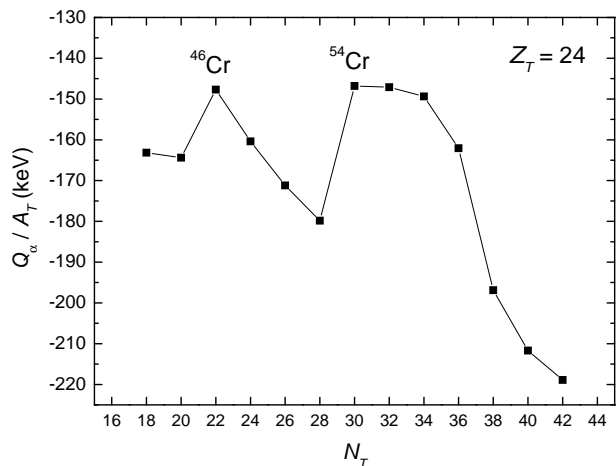


FIG. 1. Q_α/A_T values obtained for the $\alpha + \text{core}$ decomposition of even-even Cr isotopes as a function of the total neutron number N_T . The Q_α/A_T peaks corresponding to ^{46}Cr and ^{54}Cr are indicated.

simultaneously. These two Cr isotopes are then selected for a more detailed analysis in next sections.

The existence of two Q_α/A_T peaks with very close values in FIG. 1 indicates a transition from $N_{\text{core}} = 20$ to $N_{\text{core}} = 28$ as two preferential numbers for α -clustering in this mass region. However, the variation of Q_α/A_T is influenced by the changes in the nuclear shell structure for neutron-rich nuclei, and also the liquid drop behavior of the binding energy which is significant for many nuclei. For this reason, in other isotopic chains, the preferential number of neutrons of the core may vary in relation to the traditional magic numbers.

III. α -CLUSTER MODEL

The properties of the nucleus are viewed in terms of a preformed α -particle orbiting an inert core. Internal excitations of the α -cluster and the core are not considered in the calculations. The $\alpha + \text{core}$ interaction is described through a local phenomenological potential $V(r) = V_C(r) + V_N(r)$ containing the Coulomb and nuclear terms. For the nuclear potential, we adopt the form

$$V_N(r) = -V_0 \left[1 + \lambda \exp\left(-\frac{r^2}{\sigma^2}\right) \right] \left\{ \frac{b}{1 + \exp[(r-R)/a]} + \frac{1-b}{\{1 + \exp[(r-R)/3a]\}^3} \right\}, \quad (2)$$

where R and σ are free parameters and V_0 , λ , a and b are fixed parameters. The Coulomb potential $V_C(r)$ is taken to be that of a uniform spherical charge distribution of radius $R_C = R$. The inclusion of the centrifugal term results in the effective potential

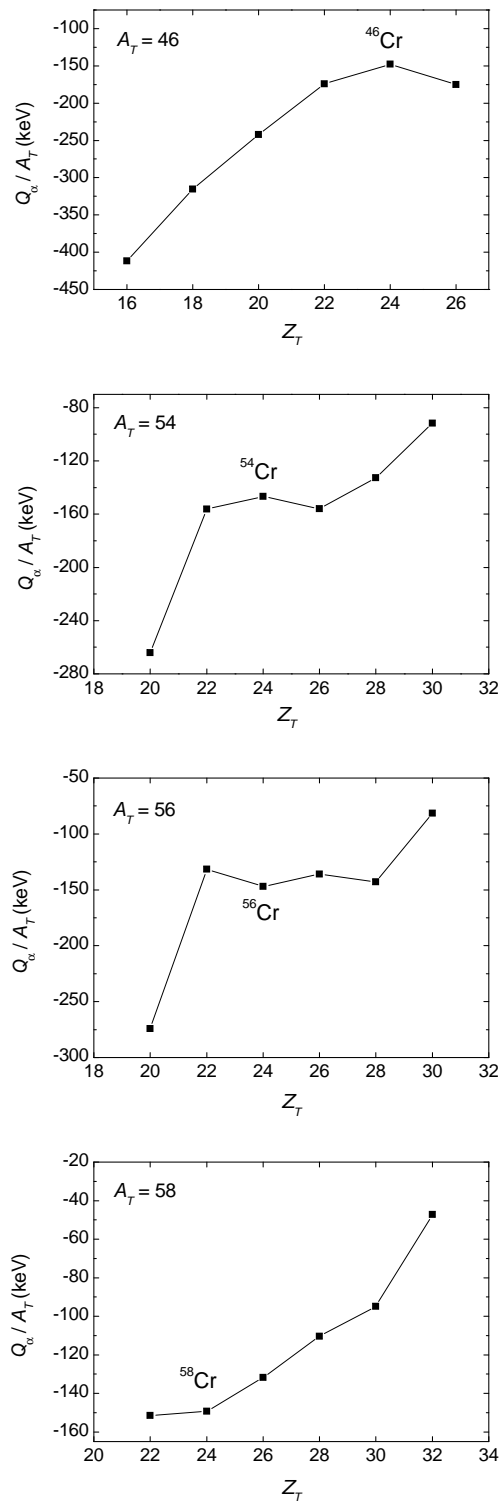


FIG. 2. Q_α/A_T values obtained for the α + core decomposition of even-even $A = 46, 54, 56, 58$ isobars as a function of the total charge number Z_T . The Q_α/A_T values corresponding to ^{46}Cr , ^{54}Cr , ^{56}Cr , and ^{58}Cr are indicated.

TABLE I. Values of the parameters R and σ for ^{46}Cr and ^{54}Cr .

Nucleus	System	R (fm)	σ (fm)
^{46}Cr	$\alpha + ^{42}\text{Ti}$	4.658	0.248
^{54}Cr	$\alpha + ^{50}\text{Ti}$	4.674	0.210

$$V_{\text{eff}}(r) = V(r) + \frac{L(L+1)\hbar^2}{2\mu r^2}, \quad (3)$$

where μ is the reduced mass of the α + core system.

The shape employed in eq. (2) is a variation of the modified Woods-Saxon potential W.S.+W.S.³. The factor of type (1 + Gaussian) allows the correct reproduction of the 0^+ bandhead, which is described roughly with the original W.S.+W.S.³ potential in previous calculations for other nuclei [5, 7]. The effect of the (1 + Gaussian) factor in the effective potential with $L > 0$ is very weak; therefore, only the 0^+ level is changed significantly in comparison with the spectrum produced by the simple W.S.+W.S.³ potential.

The ground state bands of ^{46}Cr and ^{54}Cr are calculated with the fixed values $V_0 = 220$ MeV, $a = 0.65$ fm, $b = 0.3$ and $\lambda = 0.14$, while R and σ are adjusted separately for each nucleus. The values of V_0 , a and b are the same used in Refs. [5, 7] to describe the ground state bands of nuclei of different mass regions with the W.S.+W.S.³ nuclear potential. Firstly, the parameter λ is fitted to reproduce the 0^+ bandheads of the ground state bands of ^{20}Ne , ^{44}Ti , ^{94}Mo and ^{212}Po , using the corresponding R values obtained from Ref. [5]. Then the parameters σ and R are fitted to reproduce the experimental 0^+ and 4^+ members of the ground state bands of ^{46}Cr and ^{54}Cr . (see TABLE I).

The Pauli principle requirements for the α valence nucleons are introduced through the quantum number

$$G = 2N + L, \quad (4)$$

where N is the number of internal nodes in the radial wave function and L is the orbital angular momentum. The global quantum number G identifies the bands of states. In this way, the restriction $G \geq G_{\text{g.s.}}$ is applied, where $G_{\text{g.s.}}$ corresponds to the ground state band. The value $G_{\text{g.s.}} = 12$ is employed for ^{46}Cr and ^{54}Cr . This value is obtained from the Wildermuth condition [36] considering the $(fp)^4$ configuration.

The energy levels and associated radial wave functions are calculated by solving the Schrödinger radial equation for the reduced mass of the α + core system.

IV. RESULTS

Using the α + core potential described in Section III, we have calculated the ground state bands for ^{46}Cr and

TABLE II. Calculated values of the volume integral per nucleon pair (J_R) and root-mean-square radius ($r_{\text{rms},R}$) for the $\alpha + \text{core}$ nuclear potentials employed for ^{46}Cr and ^{54}Cr .

Nucleus	System	J_R (MeV fm ³)	$r_{\text{rms},R}$ (fm)
^{46}Cr	$\alpha + ^{42}\text{Ti}$	355.0	4.314
^{54}Cr	$\alpha + ^{50}\text{Ti}$	301.1	4.323

^{54}Cr . The results are compared with the corresponding experimental energies in FIG. 3. The theoretical bands give a very good description of the experimental levels of ^{46}Cr from 0^+ to 10^+ and ^{54}Cr from 0^+ to 8^+ (uncertain assignments are indicated in FIG. 3), and a reasonable description of the higher spin levels, if we consider that the fixed parameters V_0 , a , b and λ have been adjusted to reproduce the spectra of nuclei of different mass regions. It is gratifying that the mentioned results are obtained without a dependence on quantum number L in the $\alpha + \text{core}$ potential.

According to Refs. [37–39], the experimental 0^+ , 2^+ and 4^+ levels of the ^{54}Cr g.s. band are populated in the $^{50}\text{Ti}(^6\text{Li},d)^{54}\text{Cr}$ and $^{50}\text{Ti}(^{16}\text{O},^{12}\text{C})^{54}\text{Cr}$ reactions. Such α -transfer information reinforce the choice of these states for comparison with the calculated band. However, there is no mention that the other band members are populated in the same reactions. New α -transfer experiments may be useful to confirm the spins and parities of the levels above 6^+ and verify if the levels above 4^+ are populated by these processes. It is important to observe that there are several experimental ^{54}Cr levels above $E_x \approx 4.5$ MeV which are populated in the $^{50}\text{Ti}(^{16}\text{O},^{12}\text{C})^{54}\text{Cr}$ reaction and do not have definite assignments.

It is interesting to compare the $\alpha + \text{core}$ potential of this work with optical potentials used to describe α elastic scattering. The comparison may be done through the volume integral per nucleon pair

$$J_R = \frac{4\pi}{A_\alpha A_{\text{core}}} \int_0^\infty V_N(r) r^2 dr, \quad (5)$$

and the root-mean-square (rms) radius associated with the potential

$$r_{\text{rms},R} = \left[\frac{\int_0^\infty V_N(r) r^4 dr}{\int_0^\infty V_N(r) r^2 dr} \right]^{1/2}. \quad (6)$$

Eqs. (5) and (6) refer specifically to the nuclear real part of the optical potential. TABLE II shows the J_R and $r_{\text{rms},R}$ values calculated for the nuclear $\alpha + \text{core}$ potentials of ^{46}Cr and ^{54}Cr . As usual, the negative sign of J_R is omitted.

Ref. [42] analyzes the α -particle elastic scattering at 140 MeV on ^{50}Ti using a double folding nuclear potential

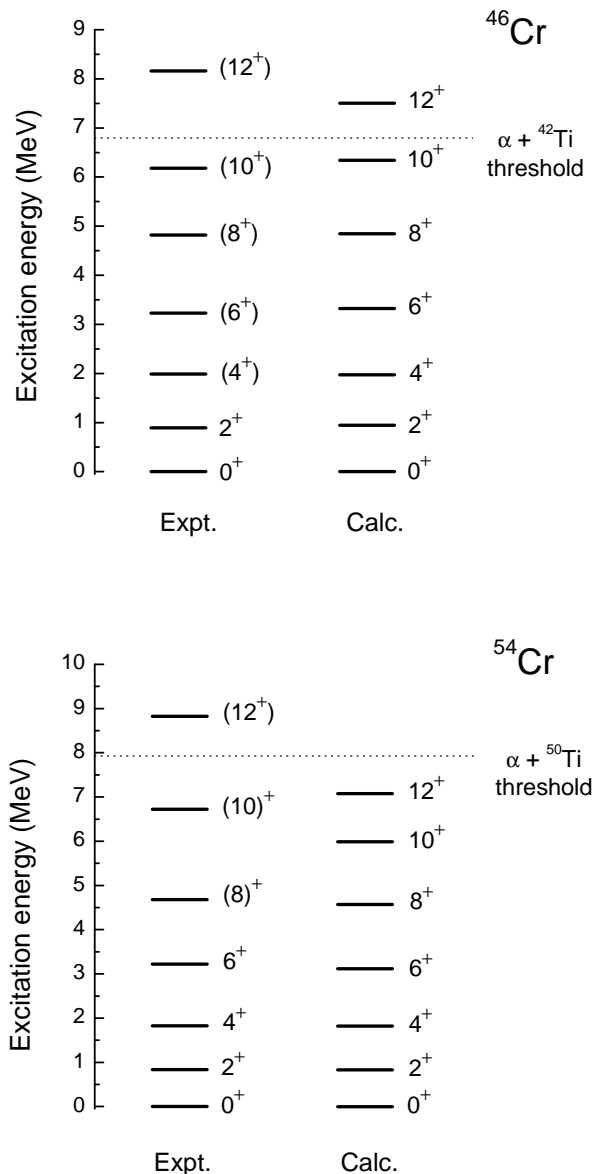


FIG. 3. Calculated $\alpha + \text{core}$ energies for the ground state bands of ^{46}Cr and ^{54}Cr in comparison with experimental excitation energies. The experimental data are from Refs. [37, 40, 41].

with DDM3Y interaction and three different shapes for the imaginary part of the optical potential; for this case, the values $J_R = 286\text{--}290$ MeV fm³ and $r_{\text{rms},R} = 4.482$ fm have been obtained. The J_R and $r_{\text{rms},R}$ values obtained in the present work for ^{54}Cr are close to the ones mentioned previously. This comparison shows there is no discrepancy between the $\alpha + \text{core}$ potential applied in this work and the real part of the optical potential of Ref. [42]. The J_R and $r_{\text{rms},R}$ values shown in the TABLE II are also compatible with the ranges obtained for the same quantities in the analysis of the α elastic scattering on ^{40}Ca at different $E_{\alpha,\text{lab}}$ energies [43].

The radial wave functions of the states have been deter-

TABLE III. Calculated values for the rms intercluster separation ($\langle R^2 \rangle^{1/2}$), the reduced α -width (γ_α^2) and the dimensionless reduced α -width (θ_α^2) for the members of the ground state bands of ^{46}Cr and ^{54}Cr . The channel radii used for the calculation of γ_α^2 and θ_α^2 are obtained from eq. (9).

^{46}Cr ($\alpha+^{42}\text{Ti}$ system)			
J^π	$\langle R^2 \rangle^{1/2}$ (fm)	γ_α^2 (keV)	θ_α^2 (10^{-3})
0^+	4.339	2.179	6.916
2^+	4.341	2.213	7.024
4^+	4.299	1.690	5.364
6^+	4.219	0.935	2.967
8^+	4.121	0.374	1.189
10^+	4.010	0.084	0.268
12^+	3.933	0.010	0.032
^{54}Cr ($\alpha+^{50}\text{Ti}$ system)			
J^π	$\langle R^2 \rangle^{1/2}$ (fm)	γ_α^2 (keV)	θ_α^2 (10^{-3})
0^+	4.290	0.631	2.184
2^+	4.290	0.637	2.205
4^+	4.249	0.471	1.630
6^+	4.181	0.268	0.927
8^+	4.089	0.101	0.350
10^+	4.003	0.027	0.092
12^+	3.933	0.003	0.011

mined to investigate other properties. A bound state approximation has been used to determine the radial wave functions of the states above the α + core threshold. For these calculations, the depth V_0 is adjusted smoothly for each state in order to reproduce the experimental excitation energies; however, the relative variation of V_0 is below 0.15 % for the states from 0^+ to 8^+ , and above 1 % only for the 12^+ state of ^{54}Cr .

The root-mean-square (rms) intercluster separation is given by

$$\langle R^2 \rangle_{G,J}^{1/2} = \left[\int_0^\infty r^2 u_{G,J}^2(r) dr \right]^{1/2}, \quad (7)$$

where $u_{G,J}(r)$ is the normalized radial wave function of a $|G, J\rangle$ state. The value of $\langle R^2 \rangle^{1/2}$ is seen to decrease when one goes from the 0^+ state to the highest spin state of each band (see TABLE III). This antistretching effect is found in nuclei of other mass regions where the α -cluster structure is studied, considering different local potential forms [5, 6, 44, 45]. Such a result shows that the inclusion of the $(1 + \text{Gaussian})$ factor in the nuclear potential does not significantly change this property in relation to the simple W.S.+W.S.³ potential.

The radial wave functions are also used for the calculation of the reduced α -width [46, 47]

$$\gamma_\alpha^2 = \left(\frac{\hbar^2}{2\mu a_c} \right) u^2(a_c) \left[\int_0^{a_c} |u(r)|^2 dr \right]^{-1}, \quad (8)$$

where μ is the reduced mass of the system, $u(r)$ is the radial wave function of the state and a_c is the channel radius. In this work, a procedure that avoids an arbitrary choice of channel radius is used. The value of a_c is given by the relation

$$a_c = 1.295(A_\alpha^{1/3} + A_{\text{core}}^{1/3}) + 0.824 \text{ (fm)}, \quad (9)$$

obtained from a linear fit [5] that considers other channel radii used for different α + core systems in the literature. The dimensionless reduced α -width θ_α^2 is defined as the ratio of γ_α^2 to the Wigner limit, that is,

$$\theta_\alpha^2 = \frac{2\mu a_c^2}{3\hbar^2} \gamma_\alpha^2. \quad (10)$$

Qualitatively, a large value of θ_α^2 (≈ 1) is interpreted as an evidence of a high degree of α -clustering.

The g.s. bands of ^{46}Cr and ^{54}Cr show a rapid decrease of γ_α^2 with the increasing spin (see TABLE III). In agreement with the analysis of the rms intercluster separations, the behavior of γ_α^2 suggests a stronger α -cluster character for the first members of these bands. For the two nuclei, the dimensionless reduced α -widths θ_α^2 present a small fraction of the Wigner limit, even for the first members of the band. This is an expected feature for strongly bound α +core states, or states above the α + core threshold and far below the top of the Coulomb barrier.

It is noted that the θ_α^2 values for ^{46}Cr are $\approx 3\times$ higher than the respective values for ^{54}Cr . The energy location of the α + core threshold has an important influence on this difference. In the excitation energy scale, the α + core threshold for ^{54}Cr is ≈ 1.1 MeV higher than the corresponding threshold for ^{46}Cr . Thus, the radial wave functions of the ^{54}Cr states are less intense in the surface region and, consequently, these states have a lower degree of α -clustering in comparison with ^{46}Cr .

The model also allows the calculation of the $B(E2)$ transition rates between the states of an α -cluster band. In the case where the cluster and the core have zero spins, this quantity is given by

$$B(E2; G, J \rightarrow J-2) = \frac{15}{8\pi} \beta_2^2 \frac{J(J-1)}{(2J+1)(2J-1)} \langle r_{J,J-2}^2 \rangle^2, \quad (11)$$

where

$$\langle r_{J,J-2}^2 \rangle = \int_0^\infty r^2 u_{G,J}(r) u_{G,J-2}(r) dr, \quad (12)$$

TABLE IV. Comparison of the calculated $B(E2)$ transition rates for the ground state bands of ^{46}Cr and ^{54}Cr with the corresponding experimental data [37, 48]. The calculated values have been obtained without effective charges.

^{46}Cr ($\alpha + ^{42}\text{Ti}$ system)		
J^π	$B(E2; J \rightarrow J-2)$ (W.u.)	$B(E2)_{\text{exp.}}$ (W.u.)
2^+	9.657	19(4) ^a
4^+	13.045	—
6^+	12.454	—
8^+	10.281	—
10^+	7.057	—
12^+	3.669	—
^{54}Cr ($\alpha + ^{50}\text{Ti}$ system)		
J^π	$B(E2; J \rightarrow J-2)$ (W.u.)	$B(E2)_{\text{exp.}}$ (W.u.)
2^+	7.456	14.4(6)
4^+	10.049	26(9)
6^+	9.688	18(5)
8^+	8.004	12.8(17)
10^+	5.729	—
12^+	2.966	—

^a Deduced from the experimental $B(E2; 0_{\text{g.s.}}^+ \rightarrow 2_1^+)$ value obtained by K. Yamada *et al.* [48].

β_2 is the recoil factor, given by

$$\beta_2 = \frac{Z_\alpha A_{\text{core}}^2 + Z_{\text{core}} A_\alpha^2}{(A_\alpha + A_{\text{core}})^2}, \quad (13)$$

$u_{G,J}(r)$ and $u_{G,J-2}(r)$ are the radial wave functions of the initial $|G, J\rangle$ state and final $|G, J-2\rangle$ state, respectively.

The calculated $B(E2)$ transition rates for the g.s. bands of ^{46}Cr and ^{54}Cr are presented in TABLE IV. A comparison of the calculated values and experimental data shows that the model can provide the correct order of magnitude of the experimental $B(E2)$ values without the use of effective charges. These results may be considered satisfactory since, in shell-model calculations for nuclei of this mass region [16, 18, 49, 50], substantial effective charges are necessary to reproduce the experimental data. Furthermore, it is shown that the calculated $B(E2)$ values for ^{54}Cr reproduce nicely the increasing or decreasing trend of the experimental data between the $2^+ \rightarrow 0^+$ and $8^+ \rightarrow 6^+$ transitions.

There are few negative parity levels with definite assignments for ^{46}Cr and ^{54}Cr , and the clear identification of negative parity bands is not possible. Nevertheless, we have calculated the 3^- level of the $G = 13$ band for a comparison with experimental energy levels of the two nuclei, applying the depth $V_0 = 238$ MeV used in the simple W.S.+W.S.³ potential for the calculation of the neg-

ative parity bands of even-even nuclei around ^{94}Mo [5]. The energies $E_{x\text{calc}}(3^-) = 3.444$ MeV and 3.258 MeV are obtained for ^{46}Cr and ^{54}Cr , respectively, to be compared with the experimental excitation energies 3.1965 MeV (uncertain assignment) and 4.12705 MeV (definite assignment), respectively. A consistent analysis of the $\alpha +$ core negative parity bands depends on further experimental data.

V. CONCLUSIONS

The calculation of Q_α/A_T values for even-even Cr isotopes and even-even $A = 46, 54, 56, 58$ isobars indicates that ^{46}Cr and ^{54}Cr are the preferential nuclei for α -clustering when compared with their even-even isotopes and isobars simultaneously. The α -cluster model gives a good account of the experimental ground state bands of these two nuclei through a local $\alpha +$ core potential with two variable parameters. The nuclear potential with $(1 + \text{Gaussian}) \times (\text{W.S.} + \text{W.S.}^3)$ shape allows the correct reproduction of the 0^+ bandheads and, additionally, describes the experimental higher spin levels of the two nuclei very well using a fixed set of four parameters which was successful in describing the ground state bands in nuclei of different mass regions.

The calculations of the volume integral per nucleon pair and rms radius show that the values for the ^{54}Cr nuclear potential are close to those obtained for the real part of the optical potential for α - ^{50}Ti elastic scattering at 140 MeV [42]. As the volume integral may vary with the $\alpha +$ core scattering energy, this comparison should not be seen as complete; however, it is shown that there is no discrepancy between the α - ^{50}Ti optical potential and the $\alpha +$ core potential of this work.

The $B(E2)$ values obtained for ^{46}Cr and ^{54}Cr give the correct order of magnitude of the available experimental data without effective charges. The calculated intercluster rms radii and reduced α -widths suggest that the α -cluster character is stronger for the first members of the ground state bands of ^{46}Cr and ^{54}Cr . Therefore, the use of the $(1 + \text{Gaussian})$ factor in the $\alpha +$ core nuclear potential does not change significantly this feature as compared to other $\alpha +$ core calculations in different mass regions.

New experimental data, especially from α -transfer reactions, will be important to complement the analysis of this work.

ACKNOWLEDGMENTS

The authors thank the members of the Nuclear Spectroscopy with Light Ions Group of University of São Paulo for the productive discussions. This work was financially supported by Coordenação de Aperfeiçoamento de Pessoal de Nível Superior (CAPES).

-
- [1] H. Horiuchi, K. Ikeda, and K. Katō, *Prog. Theor. Phys. Suppl.* **192**, 1 (2012).
- [2] C. Beck, *Journal of Physics: Conference Series* **569**, 012002 (2014).
- [3] B. Buck, A.C. Merchant, and S.M. Perez, *Few-Body Systems* **29**, 53 (2000).
- [4] B. Buck, A.C. Merchant, and S.M. Perez, *Nucl. Phys.* **A657**, 267 (1999).
- [5] M.A. Souza and H. Miyake, *Phys. Rev. C* **91**, 034320 (2015).
- [6] F. Michel, G. Reidemeister, and S. Ohkubo, *Phys. Rev. C* **37**, 292 (1988).
- [7] B. Buck, A.C. Merchant, and S.M. Perez, *Phys. Rev. C* **51**, 559 (1995).
- [8] A.C. Merchant, K.F. Pál, and P.E. Hodgson, *J. Phys. G: Nucl. Part. Phys.* **15**, 601 (1989).
- [9] S. Ohkubo, Y. Hirabayashi, and T. Sakuda, *Phys. Rev. C* **57**, 2760 (1998).
- [10] F. Michel, S. Ohkubo, and G. Reidemeister, *Prog. Theor. Phys. Suppl.* **132**, 7 (1998).
- [11] A.C. Merchant, *J. Phys. G: Nucl. Phys.* **10**, 885 (1984).
- [12] A.C. Merchant, *Phys. Rev. C* **36**, 778 (1987).
- [13] T. Sakuda and S. Ohkubo, *Phys. Rev. C* **51**, 586 (1995).
- [14] T. Sakuda and S. Ohkubo, *Phys. Rev. C* **57**, 1184 (1998).
- [15] Y. Taniguchi, *Prog. Theor. Exp. Phys.* **2014**, 073D01 (2014).
- [16] K. Kaneko, Y. Sun, M. Hasegawa, and T. Mizusaki, *Phys. Rev. C* **78**, 064312 (2008).
- [17] T. Togashi, N. Shimizu, Y. Utsuno, T. Otsuka, and M. Honma, *Phys. Rev. C* **91**, 024320 (2015).
- [18] J. Kotila and S.M. Lenzi, *Phys. Rev. C* **89**, 064304 (2014).
- [19] K. Sato, N. Hinohara, K. Yoshida, T. Nakatsukasa, M. Matsuo, and K. Matsuyanagi, *Phys. Rev. C* **86**, 024316 (2012).
- [20] H. Oba and M. Matsuo, *Prog. Theor. Phys.* **120**, 143 (2008).
- [21] S. Saini and M.R. Gunye, *Phys. Rev. C* **24**, 1694 (1981).
- [22] B. Banerjee, S.B. Khadkikar, and K.R. Sandhya Devi, *Phys. Rev. C* **7**, 1010 (1973).
- [23] P. Descouvemont, *Nucl. Phys.* **A709**, 275 (2002).
- [24] T. Sakuda and S. Ohkubo, *Nucl. Phys.* **A712**, 59 (2002).
- [25] F. Wienholtz *et al.*, *Nature* **498**, 346 (2013).
- [26] A. Gade *et al.*, *Phys. Rev. C* **74**, 021302(R) (2006).
- [27] R.V.F. Janssens *et al.*, *Phys. Lett. B* **546**, 55 (2002).
- [28] D.-C. Dinca *et al.*, *Phys. Rev. C* **71**, 041302(R) (2005).
- [29] A. Bürger *et al.*, *Phys. Lett. B* **622**, 29 (2005).
- [30] J.I. Prisciandaro *et al.*, *Phys. Lett. B* **510**, 17 (2001).
- [31] D. Steppenbeck *et al.*, *Nature* **502**, 207 (2013).
- [32] C.F. Jiao, J.C. Pei, and F.R. Xu, *Phys. Rev. C* **90**, 054314 (2014).
- [33] H.L. Crawford *et al.*, *Phys. Rev. Lett.* **110**, 242701 (2013).
- [34] G. Audi, M. Wang, A.H. Wapstra, F.G. Kondev, M. MacCormick, X. Xu, and B. Pfeiffer, *Chinese Physics C* **36**, 1287 (2012); <http://amdc.in2p3.fr/web/masseval.html>
- [35] M. Wang, G. Audi, A.H. Wapstra, F.G. Kondev, M. MacCormick, X. Xu, and B. Pfeiffer, *Chinese Physics C* **36**, 1603 (2012); <http://amdc.in2p3.fr/web/masseval.html>
- [36] K. Wildermuth and Y.C. Tang, *A Unified Theory of the Nucleus* (Academic Press, New York, 1977).
- [37] Yang Dong and Huo Junde, *Nuclear Data Sheets* **121**, 1 (2014).
- [38] H. Faraggi, M-C. Lemaire, J-M. Loiseaux, M.C. Mermaz, and A. Papineau, *Phys. Rev. C* **4**, 1375 (1971).
- [39] H.W. Fulbright *et al.*, *Nucl. Phys.* **A284**, 329 (1977).
- [40] Balraj Singh, *ENSDF Database*: <http://www.nndc.bnl.gov/ensdf/>
- [41] S.-C. Wu, *Nucl. Data Sheets* **91**, 1 (2000).
- [42] A.M. Kobos, B.A. Brown, P.E. Hodgson, G.R. Satchler, and A. Budzanowski, *Nucl. Phys.* **A384**, 65 (1982).
- [43] U. Atzrott, P. Mohr, H. Abele, C. Hillenmayer, and G. Staudt, *Phys. Rev. C* **53**, 1336 (1996).
- [44] B. Buck, C.B. Dover, and J.P. Vary, *Phys. Rev. C* **11**, 1803 (1975).
- [45] S. Ohkubo, *Phys. Rev. Lett.* **74**, 2176 (1995).
- [46] A. Arima and S. Yoshida, *Nucl. Phys.* **A219**, 475 (1974).
- [47] G. Michaud, L. Scherk, and E. Vogt, *Phys. Rev. C* **1**, 864 (1970).
- [48] K. Yamada *et al.*, *Eur. Phys. J. A* **25**, s01, 409 (2005).
- [49] K. Langanke, D.J. Dean, P.B. Radha, Y. Alhassid, and S.E. Koonin, *Phys. Rev. C* **52**, 718 (1995).
- [50] K. Itonaga, *Prog. Theor. Phys.* **66**, 2103 (1981).